Transnational University Limburg is a unique collaboration of two universities in two countries: the University of Hasselt and Maastricht University.

UHASSELT
KNOWLEDGE IN ACTION

www.uhasselt.be
Universiteit Hasselt
Campus Hasselt:
Martelarenlaan 42 | 3500 Hasselt
Campus Diepenbeek:
Agoralaan Gebouw D | 3590 Diepenbeek

UHASSELT
KNOWLEDGE IN ACTION

Maastricht University

Faculty of Medicine and Life Sciences
School for Life Sciences

Master of Biomedical Sciences

Masterthesis

Radiation exposure during posterior lumbar intervertebral fusion procedures, using intraoperative CT versus conventional C-arms

Elien Houben

Thesis presented in fulfillment of the requirements for the degree of Master of Biomedical Sciences, specialization Clinical Molecular Sciences

SUPERVISOR :
Prof. dr. Ivo LAMBRICHTS
Prof. Dr. Jan VANDEVENNE

CO-SUPERVISOR :
Dr. Sofie VAN CAUTER

2017
2018

UHASSELT
KNOWLEDGE IN ACTION

Maastricht University

Faculty of Medicine and Life Sciences
School for Life Sciences
Master of Biomedical Sciences

Masterthesis

Radiation exposure during posterior lumbar intervertebral fusion procedures, using intraoperative CT versus conventional C-arms

Elien Houben

Thesis presented in fulfillment of the requirements for the degree of Master of Biomedical Sciences, specialization Clinical Molecular Sciences

SUPERVISOR :
Prof. dr. Ivo LAMBRICHTS
Prof. Dr. Jan VANDEVENNE

CO-SUPERVISOR :
Dr. Sofie VAN CAUTER

Acknowledgments

I would first like to thank the University of Hasselt for the opportunity it has given me to become a biomedical scientist. Throughout my Bachelor and Master, professors and PhD students have taught us to think critically and supplied us with the proper knowledge.

Secondly, I would like to acknowledge Prof. dr. Ivo Lambrichts of the Morphology department at Hasselt University as my institutional supervisor and Prof. dr. Sven Hendrix of the Morphology department at the Hasselt University as the second reader of this thesis. I am gratefully indebted to them for their valuable comments on this thesis.

I would also like to thank Ziekenhuizen Oost-Limburg for the opportunity to do my senior training at their institution of Campus Sint-Jan. Thereby; I would like to thank Prof. Dr. Jan Vandevenne from the department of Medical Imaging at ZOL as my principle supervisor, for allowing me to conduct this study. A very special thanks to my daily supervisor Dr. Sofie Van Cauter of the department of Medical Imaging at ZOL. She consistently allowed this paper to be my own work, but steered me in the right the direction whenever she thought I needed it.

Next, I would like to thank the department of Neurosurgery with mention of the neurosurgeons who were involved in this research project; Dr. Eveleen Buelens, Dr. Thomas Daenekindt and Dr. Dieter Peuskens. Without their passionate participation, the study could not have been successfully conducted. Besides, I would like to thank the OR staff and secretaries of the department of Neurosurgery.They were always willing to help me with the study.

I am grateful for the help of dr. Albrecht Houben, radiation physicist at Ziekenhuizen Oost-Limburg. His door was always open whenever I ran into a problem or had a question about my research or writing.

I would also like to thank the staff of LCRP for supplying me with a desk at their department. With a special mention of dr. ir. Inge Thijs, who arranged a lot for me, dr. Christophe Smeets, who gave me a lot of advice and was a listening ear, and Ward Eertmans for the help with my statistical analysis.

Finally, I must express my very profound gratitude to my friends and family for providing me with unfailing support and continuous encouragement throughout my years of study and through the process of researching and writing this thesis. This accomplishment would not have been possible without them. Thank you.

Content

List of abbreviations

2D	Two-dimensional
3D	Three-dimensional
ALARA	As Low As Reasonably Achievable
ALIF	Anterior Lumbar Interbody Fusion
AP	Anterior-Posterior
ARBIS	General regulations for the protection of the population, workers and the environment against the danger of ionizing radiation (translated from Dutch)
ATP	Anterior To Psoas
BMI	Body Mass Index
cm	Centimeter
CTDI	Computed Tomography Dose Index
DAP	Dose Area Product
DLP	Dose Length Product
ED	Effective Dose
FANC	Federal Agency for Nuclear Control
Gy	Gray
H	Dose Equivalent
H_T	Tissue-Weighted Dose Equivalent
ICRP	International Comisson on Raliological Protection
iCT	Intraoperative Computed Tomography
kV	Kilovolt
L	Lateral
LLIF	Lateral Lumbar Interbody Fusion
mA	Milliampere
mAs	Milliampere-second
MI-PLIF	Minimal Invasive Posterior Lumbar Interbody Fusion
MIS	Minimal Invasive Surgery
OLIF	Oblique Lumbar Interbody Fusion
PLIF	Posterior Lumbar Interbody Fusion
PSD	Peak Skin Dose
SI	International System
SPSS	Statistical Package for Social Sciences
Sv	Sievert
W_R	Weighting Factor
W_T	Tissue-Weighting Factor
XLIF	Extreme Lateral Interbody Fusion

Abstract

Introduction: Minimal invasive posterior lumbar interbody fusion procedures can be performed with the help of imaging devices used for navigation. C-arm fluoroscopy is the current gold standard, while intraoperative CT allows for navigation and orientation in three dimensions. Due to the novelty, intraoperative CT is still poorly studied in navigation during PLIF. The main problem with the use of X-ray imaging techniques is the dose of ionizing radiation to patients and staff. In this study, we aim to investigate the radiation exposure of iCT versus biplanar C- arms during MI-PLIF procedures.

Material & methods: Patients with MI-PLIF of less then three levels were consecutively included from November 2016 to June 2018. The Fluorostar 7900 series C-arm and Airo® intraoperative CT were used as navigation devices during these procedures. We determined patients' peak skin dose with Gafchromic™ films and effective dose with a conversion factor, obtained from a Monte Carlo simulation. The effective dose incurred by staff was measured with Philips DoseAware dosimeters. To evaluate the efficiency, we measured two time intervals. Statistical analysis was performed a student T-test or Mann-Whitney U test to compare normally and not normally distributed continuous data, retrospectively ($p<0.05$).

Results: We studied 57 procedures. Analysis of the peak skin dose of patients revealed a significant higher dose on the patient's lateral side with the use of C-arm fluoroscopy compared to iCT. The effective dose of patients was significantly higher for intraoperative CT compared to C-arm fluoroscopy. However, the effective dose of staff was significantly lower with intraoperative CT for the surgeon and scrub nurse. The operation time was significantly longer for intraoperative CT in both time intervals.

Discussion & conclusion: The present data indicate that iCT has a larger radiation area with a lower localized dose, while C-arm fluoroscopy results in a localized radiation area with a higher focal dose. The ED of the patient with iCT increased by fourfold compared with the conventional biplanar C-arms. However, the ED for the surgeon was almost 17 times lower and 6 times lower for the nurse in the iCT group. For the evaluation of the full operation length, the average difference was one hour between both groups. When solely evaluating the duration for the screw placement, the procedure performed with iCT was on average 37 minutes longer than the procedure with fluoroscopy. In conclusion, the iCT is an interesting neuronavigation device for operating personnel to reduce and possibly eliminate radiation exposure in MI-PLIF procedures. However, adjustments can be made to lower the patient's dose and staff could be trained to overcome the learning curve of the Airo® iCT.

1 Introduction

Spinal disorders such as spondylolisthesis, spinal stenosis or discopathy are common conditions, which have a considerable impact on daily life. They cause pain or weakness in the lower limbs and back, which are the top global causes of disability (1-3). Treatment for these entities consists primarily of conservative treatment and physical therapy. If conservative treatment fails to relieve pain and discomfort, surgery can be considered. One surgical treatment option is the fusion of vertebrae to stabilize the spine, in order to decompress the nerves (1, 2, 4).

1.1 Lumbar intervertebral fusions

In a lumbar fusion procedure, the spine can be approached from an anterior, anterolateral, lateral, posterolateral and posterior surgical standpoint (Fig. 1B). Each approach has its advantages and disadvantages and therefore the choice of approach is case-depended. For example, the anterior approach is better to restore lordosis, while the posterior approach is superior for treating stenosis of the central canal, spondylolisthesis or recurrent disc herniations (2).

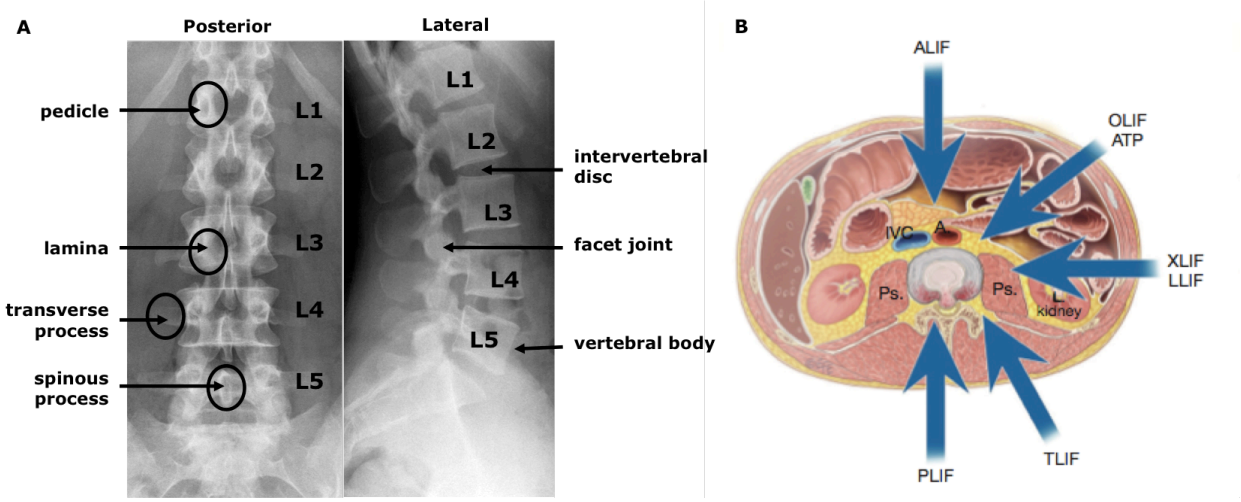

Figure 1: Surgical approaches to the lumbar spine for interbody fusion techniques. (A) Radiographic images of the compounds of the lumbar spine with a lordotic curvature. **(B)** The five interbody fusion approaches during vertebral fusion: anterior (ALIF), oblique lumbar interbody fusion/ anterior to psoas (OLIF/ATP), lateral or extreme lateral interbody fusion (LLIF or XLIF), transforaminal (TLIF), and posterior (PLIF). (Adapted from "Lumbar interbody fusion: techniques, indications and comparison of interbody fusion options including PLIF, TLIF, MI-TLIF, OLIF/ATP, LLIF and ALIF," by Author R.J. Mobbs, 2015, *Journal of Spine Surgery, 1*(1):2-18) (2)

1.1.1 Posterior lumbar interbody fusion

The posterior lumbar interbody fusion (PLIF) procedure aims to decompress the nerves in the spinal canal and fuse the vertebrae in order to stabilize the spine. This technique allows for a restoration of interbody discus height between the vertebrae (2). The traditional open spine approach is associated with prolonged muscle retraction during surgery and frequently entails damage to the neurovascular structures supplying the intrinsic muscles of the spine. As a result, a long hospital stay and postoperative complications are common. For this reason, minimal invasive surgery (MIS) has been developed, using smaller incisions implying less manipulation of nerve and muscle tissue. This results in a reduced rehabilitation period, less postoperative pain and fewer complications (1, 2, 5).

1.1.2 Minimal invasive PLIF

During a minimal invasive PLIF (MI-PLIF) surgery, screws are placed in the pedicles (Fig. 1A) of the lower and upper vertebra of the intervertebral space of interest (Fig. 2A). The screws are inserted through small incisions approximately five centimeters laterally from the midline incision. After placement of the screws, rods are placed through the same lateral incisions (Fig. 2B). These rods can be fixed on the screws and afterwards the surgeon manipulates these rods in order to distract or compress the vertebrae to restore listhesis and the lordotic curvature of the lumbar spine (Fig. 1A). Thereafter, the spinous process, facet joints and/or lamina (Fig. 1A) are removed through a midline incision to decompress the nerves. After removal of the intervertebral disc, the cages are placed in between the vertebrae. If there is space left between the vertebrae, remaining bone graft can be placed to promote bone growth in order to optimize the vertebral fusion (Fig. 2C) (5-7).

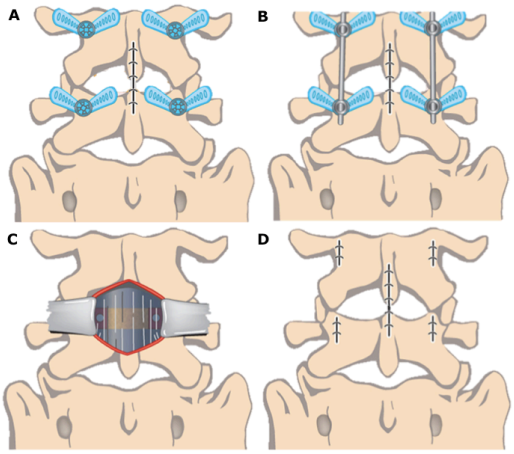

Figure 2: Schematic diagram of a MI-PLIF procedure. (A) Phase I, pedicle screw placement. **(B)** Phase I placement of rods. **(C)** Phase II, neuronal decompression by removal of processus spinosus and facet joints, followed by phase III, discectomy and insertion interbody cages through the medial incision. Thereafter, compression of the vertebral bodies in phase IV. **(D)** Closure of lateral and medial incisions. (Adapted from "Minimally invasive surgery compared to open spinal fusion for the treatment of degenerative lumbar spine pathologies," by Author R.J. Mobbs, 2012, *Journal of Clinical Neuroscience, 19*: 829–835) (5)

1.2 X-ray based imaging devices

In order to help surgeons navigate with the placement of the pedicle screws and graft cages during a MI-PLIF procedure, X-ray based imaging techniques are used. In this study the focus will be on two imaging techniques used during these surgical procedures: C-arm fluoroscopy and intraoperative computer tomography (iCT).

1.2.1 Principles of diagnostic radiography

X-rays are generated in a vacuum tube where electrical energy is converted into ionizing radiation. The photons of the X-ray beam are sent through the patient from the X-ray tube to the detector. Thereby, three physical interactions can occur with the patient on atomic level: transmission, absorption and scattering. The detector captures the X-rays that didn't interact with matter, a phenomenon called transmission. In case the photon interacts with the tissue of the patient, the photon transmits its energy to the electrons of the atom of interaction. The energy of the photon can be completely or incompletely absorbed. In case of incomplete absorption, the photon will divert from its initial direction with lower energy. This is called scattering and is a cause of secondary radiation. The interaction with matter will be further clarified in section 1.2.4 (8, 9).

X-rays can be used for diagnostic purposes by creating an image based on the X-rays captured by the detector. The gray scale on the image is an indication of how many X-rays interacted with the patient. For example, bone attenuates almost all X-rays and is therefore displayed in white. In contrast to bone, all X-rays pass through air and will result in a black X-ray density. Soft tissue has a gray scale in between, depending on the interaction of the X-rays. This attenuation of the X-ray beam will lead to an accurate image of the anatomy (10).

1.2.2 C-arm fluoroscopy

The current gold standard during a PLIF procedure is the use of biplanar C-arms. These devices consist of a mobile unit with a C-arm attached that contains an X-ray generator and a detector on the opposite site (Fig. 3). This C-arm is rotatable in three directions. It can rotate in a vertical-horizontal manner to the left and right with a range of 225° and has an orbital motion of 120°. The third motion is a right to left rotation of 10° on its column. The image created by the X-rays on the detector, is projected on an additional monitor cart as shown in Figure 3 (11).

C-arm fluoroscopy is used in a wide range of surgical procedures where surgeons are in need of guidance during the placement of foreign object into the body. For example, it is often used in the field of endoscopy, neurology, cardiology and urology for stenting or drainage procedures. Moreover, C-arms are used for screw placement in orthopedic and neurosurgical procedures such as vertebral fusions (12).

During a MI-PLIF procedure, two C-arm devices are placed in a lateral and anterior-posterior (AP) manner, which results in two two-dimensional images (Fig.3). Hence, an anterior-posterior and lateral (L) image of the spine allows the surgeon to visualize the position of the instrument based on two perpendicular directions. Since, an anterior-posterior direction is used, the X-ray beam has to pass through the table. Therefore, a radiolucent table is necessary. The advantages of this approach are the low cost and the availability of the different beam angles because of the possibility to reposition the arm of the device (6).

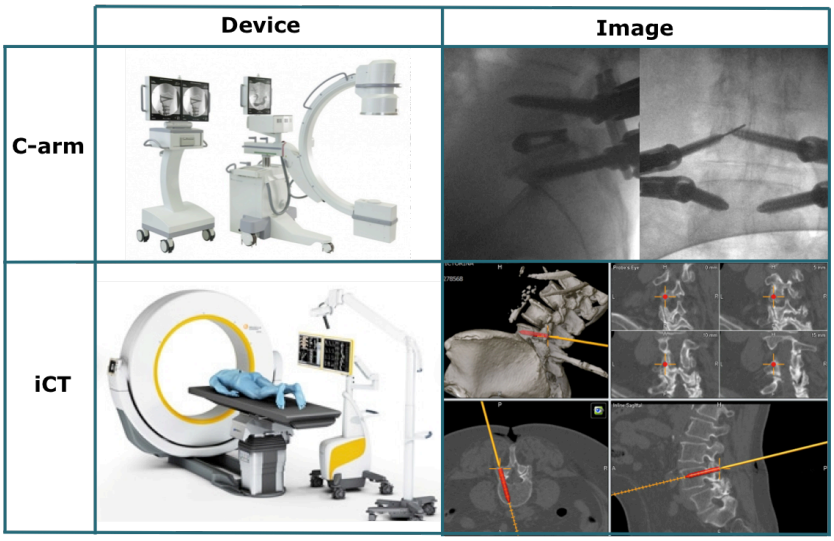

Figure 3: Imaging techniques during MI-PLIF surgery. In the first row, the device of the Fluorostar 7900 series C-arm is shown with on the right panel the lateral and anterior-posterior 2D-images it creates. The second row shows the set-up of the Airo® iCT with the Curve™ neuronavigation control center on the left panel, and the images with neuronavigation as projected during procedure on the right panel (11, 13-15).

1.2.3 Intraoperative CT

An intraoperative CT (iCT) is a recently developed mobile imaging device, which allows the generation of CT images in the operating theater during a surgical procedure. The iCT used in this study is called Airo®, developed by Brainlab in 2013 and is installed in the operating theater of Ziekenhuizen Oost-Limburg, Campus St. Jan Genk since November 2015.

Airo® is mobile donut shaped imaging device placed on a rail in the operating theater (Fig. 3). During the surgical procedure, the CT moves over the radiolucent table and performs a scan of the area of interest. The full spine can be imaged in one step. The large gantry of 107 cm and the large field of view are adapted to the intraoperative use. Airo® CT is a third generation CT scanner; meaning that the X-ray fan beam and detector are simultaneously rotating during image acquisition. The detector allows the acquisition of 32 slices per rotation. As a comparison, current clinical CT scanners in the medical imaging department allow the acquisition of up to 384 slices per rotation. The apparent limitations of the Airo® CT are because of the need for transport in the operating theater, which necessitate a smaller, lighter and mobile imaging device (14, 15).

Furthermore, the Airo® communicates with a control and information center called Curve™ (Fig.3). This system consists of an infrared camera and workstation with neuronavigation software, allowing the surgeon to determine the spatial position of the instruments during surgery. According to the meta-analysis of Meng X.T. *et al.*, this leads to a significantly higher accuracy of the placement of the pedicle screws (6). Moreover, the Airo® CT allows real-time 3D and cross-sectional reconstruction of images. Regarding radioprotection issues, the radiation dose of the Airo® CT can be adjusted by selecting one of several scan protocols. These protocols minimize the image noise by adjusting the tube current based on the patients weight and anatomy. Each scanning protocol is optimized for a certain part of the body to provide an optimized dose for equivalent image quality. In order to further reduce the radiation dose, different percentages of the tube current can be chosen (13-16).

1.3 Radiation Exposure

As briefly discussed in section 1.2.2, X-rays consist of photons that interact with matter on an atomic scale. There are three main interactions that are of importance for diagnostic radiation: absorption, scattering and transmission as shown in Figure 4.

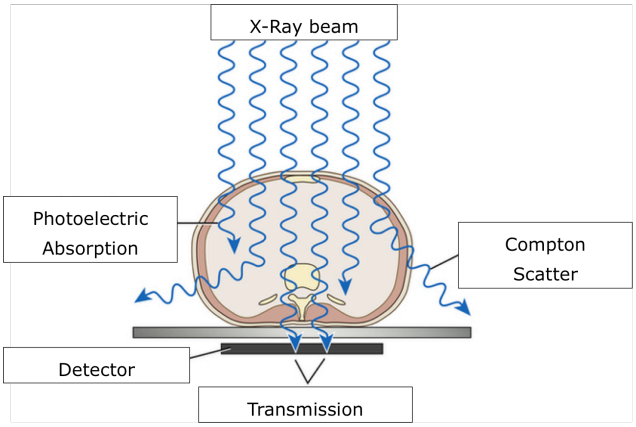

Figure 4: Attenuation of the X-ray beam. The X-ray beam interacts with the patient, whereby X-ray photons are absorbed, scattered or transmitted. The attenuated X-ray beam is the product of absorption and

scatter, and will be detected. (Adapted from "Radiologykey (2016, Feb 27) *Image production*. Retrieved from https://radiologykey.com/image-production/")(17)

The first interaction of interest is the absorption of an X-ray photon by an atom in the tissue of the patient. This effect is called photoelectric effect and will contribute to the attenuation of the initial X-ray beam (Fig. 5A). During this phenomenon, the initial photon will interact with a photon on the inner shell of the atom if the energy of the initial photon is higher than or equal to the binding energy of the electron on the inner shell of the atom. This interaction will result in ejection of the electron from its orbit. An electron on the outer shell of the atom can then fill the gap with emission of characteristic radiation in order to lose energy. The characteristic radiation will not directly contribute to the image since it doesn't leave the body. However, it can contribute to secondary ionizations, which are important for safety hazards. Taken together, this photoelectric effect will result in characteristic radiation, a photoelectron and a positive ion (9, 18).

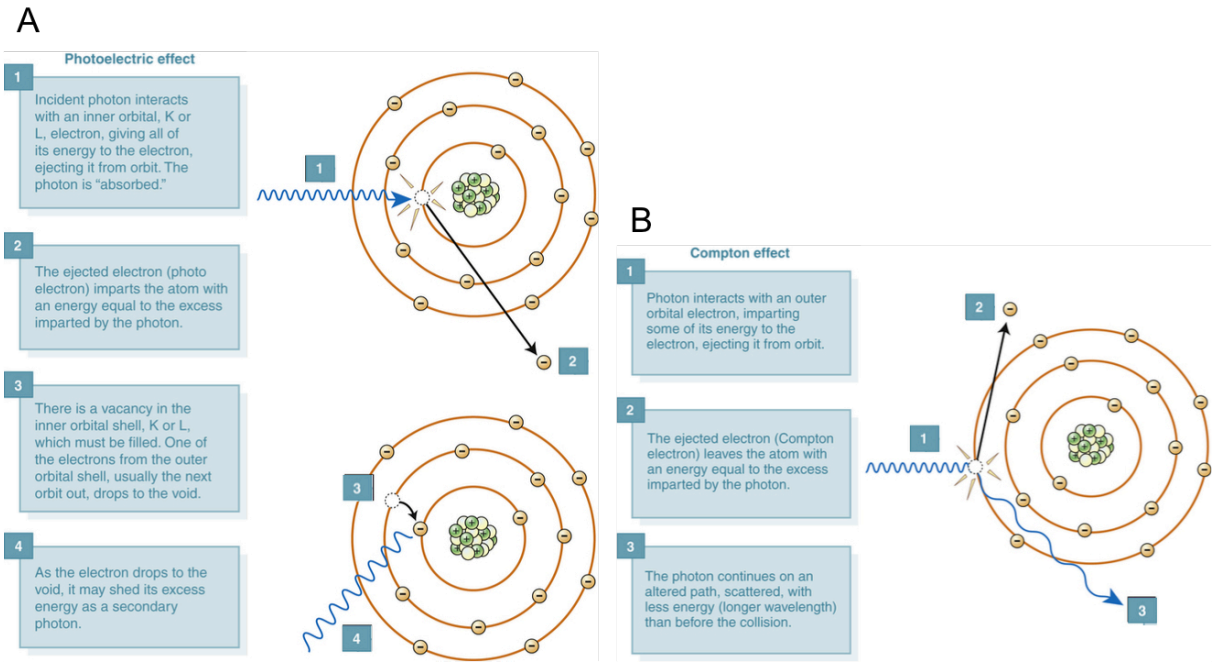

Figure 5: The atomic interactions of the X-ray beam with tissue. (A) The Photoelectric Effect, representing the absorption of the photons from X-ray beam. **(B)** The Compton Effect, representing the scatter radiation. (Adapted from "Radiologykey (2016, Feb 27) *Image production*. Retrieved from https://radiologykey.com/image-production/")(17)

The other interaction contributing to the attenuation of the initial X-ray beam is scattering. The scatter interaction is defined as the Compton effect and will interact with an electron on the outer shell of the atom (Fig. 5B). This effect will occur if the energy of the initial photon equals the binding energy of the electron in the outer shell of the atom. The initial photon will then push the electron out of its shell and deflect in a different direction as scatter radiation. This photon will retain most of its energy and therefore be the main effect for safety hazards with X-ray radiation. Moreover, this scatter radiation can scatter in every angle and will be of great importance in this study, since this is the radiation the staff will be exposed to. On the other hand, the recoil electron and positive ion that result from this interaction are important for the harmful effect of secondary ionization in the patient (9, 18).

To conclude, the attenuation of the X-ray beam is a product of the adsorption and scatter interactions. This attenuation is depended on the difference in atomic number and mass density in tissue. For example, bone has a higher atomic number then fat, resulting in more photoelectric absorption and leading to a lighter image density. The mass density plays a role in the probability of the X-ray photon interacting with an atom, e.g. when comparing bone with air (10).

1.3.1 Biological effects of ionizing radiation

As mentioned above, the interactions result in the formation of negative electrons, positive atoms and characteristic radiation. These factors contribute to the biological effects the X-ray radiation has and is therefore called ionizing radiation. There are four biological reactions that can occur. The first interaction is previously discussed and occurs when the initial X-ray photon ionizes the atom it interacts with. This interaction can lead to secondary radiation when the ejected electron has sufficient energy to cause ionization in other atoms of the tissue. This can results in a direct effect by breaking of weak organic bindings or an indirect effect by radiolysis. The direct effect will lead to changes in the structure of the cell, while the indirect effect will lead to the formation of highly reactive radicals from water molecules. These radicals can interact with molecules of the cell such as DNA. Overall this will result in chemical changes and possibly induce biological damage (8, 9).

The biological effect of ionizing radiation as a result of damage to cell structures and DNA are DNA breaks, cross linking of vital molecules and damage to the nitrogen bases of the DNA. The cell damage results in deregulated cellular processes, causing the cell to react in three different ways. First, repair mechanisms are activated to restore the DNA damage. However, the repair mechanisms of the cell are not always successful and misrepair or non-repair can occur. Double strand breaks often lead to an increased risk of cancer development, since they are the most difficult to repair. If repair mechanisms fail, the cell can be modified by gene mutations or chromosome aberrations. These modified cell types have very unstable genetic material. The third cellular response is cell death by programmed apoptosis (8).

1.3.2 Classification of biological effects

The area of the damage, the time of observable clinical effects and the nature of the effect classify the biological effects of ionizing radiation. The damaged area is categorized in somatic or genetic effects. The somatic effect can occur in an acute, sub-acute or late phase, while the genetic effect refer to the hereditary effect and will occur later in the offspring (8, 9).

These effects were recently re-categorized by the nature of the effect. Deterministic effects are referred to as functional disorders and can occur if a patient is exposed to a radiation dose above a certain threshold. These effects will occur with certainty and increase in severity with an increase in radiation dose. Examples of deterministic effects are hair loss, erythema or changes in the blood composition. Meanwhile, stochastic effects will occur with an increased probability if the radiation dose increases. However, these stochastic effects are random and have no safe dose limit since all doses carry a risk. Furthermore, the severity of the effects is not dependent on the radiation dose with stochastic effects. These effects can give rise to radiation-induced cancers and genetic defects (9).

1.3.3 Dosimetry

There are several International System (SI) units to quantify the doses patients are exposed to. In order to measure the radiation dose patients absorbed, the energy transferred by the ionizing radiation per unit is divided by the irradiated mass. This unit is expressed in Gray (Gy). However, to encounter the biological effect of the radiation dose, a dose equivalent (H) is defined. The SI unit for the equivalent dose is Sievert (Sv). To simplify, the SI unit Gray is used for physical quantification, while the SI unit Sievert is used to quantify the biological effect. To modify the absorbed dose to the dose equivalent, taking the type of radiation into account, the International Commission on Radiological Protection (ICRP) establishes a weighting factor (W_R). Since tissue can differ in radiation sensitivity, different tissue weighting factors (W_T) are defined by the ICRP. The effective dose (ED) is a tissue-weighted sum of the dose equivalent (H_T) and the corresponding weighting factor for that specific organ or tissue. The effective dose represents the stochastic effect of the whole body. Likewise, this dose is expressed in Sievert (10, 18)

1.3.4 Radiation protection

The ICRP introduced the ALARA principle in 1997 stating that radiation doses to patients and staff should be kept as low as reasonably achievable (ALARA). In Belgium, the Federal Agency for Nuclear Control (FANC) published the royal decree of July 20th 2001 (ARBIS), in which effective dose limits are described in Chapter III, Article 20. For staff the effective dose limit is 20 mSv for twelve consecutive months and for the public the limit is 1 mSv per year (19).

1.4 Goal of the study

In this study, we wanted to evaluate the use of a new imaging technique, the intraoperative CT during a MI-PLIF procedure and compare this to the gold standard, C-arm fluoroscopy. These imaging techniques are used because surgeons are in need of guidance to facilitate an accurate placement of the surgical instruments in a minimal invasive procedure. While performing a MI-PLIF procedure, patient and staff are exposed to ionizing radiation due to the use of these X-ray based imaging devices. Since the newly developed iCT is still poorly studied regarding radiation protection, the aim of this study is to investigate the radiation dose of iCT versus biplanar C-arms during MI-PLIF procedures. We hypothesize that the iCT has a lower radiation dose for staff, but an equal or higher radiation dose for patients in comparison to the biplanar C-arms. To test this hypothesis, the peak skin dose and effective dose of patients and the effective dose of staff will be quantified. In order to evaluate the efficiency of both techniques, the operation length will be measured.

2 Material and methods

The ethical commissions of Ziekenhuizen Oost-Limburg and Hasselt University approved this study on January 17th, 2017. The study was a cooperation of the department of Medical Imaging and Neurosurgery. Patients who underwent a MI-PLIF with the use of the Airo® iCT or biplanar C-arms at Ziekenhuizen Oost-Limburg, Campus St. Jan between November 2016 and June 2018 were included in a consecutive manner. The senior intern enrolled the patients after providing them with an informed consent. Data was included in the analysis if the procedures fulfilled the inclusion and exclusion criteria described in the next section. The procedures were conducted by three neurosurgeons specialized in spinal fusions, whereby surgeon 1 has 11 years of experience, surgeon 2 has 16 years of experience and surgeon 3 has 19 years of experience. Patients' demographic data, surgical indications, level of fusion were prospectively recorded.

2.1 Inclusion criteria

Patients were included when there was compliance with the following criteria: full informed consent, older than 18 years, eligible for a full PLIF procedure with screw fixation and cage placement and with a fusion of less than three levels. The use of other devices was not allowed during the studied procedures.

2.2 Materials

The imaging devices used in the study are the C-arm OEC Fluorostar 7900 series (GE Healthcare, Little Chalfont, UK) compared with the intraoperative Airo® iCT (Mobius Imaging, Shirley, Massachusetts, USA). These devices were placed over a radiolucent table (TRUMPF TruSystem 7500, Trump Medical, Saalfeld, Germany). The Airo® iCT is connected to a navigation workstation with navigation software called Curve™ (Brainlab AG, Munich, Germany). To measure the radiation dose of the staff during the procedures, personnel dosimeters from the DoseAware System (Philips, Amsterdam, The Netherlands) were used. The peak skin dose of the patient was measured with Gafchromic™ XR-RV3 (Ashland Inc., Covington, Kentucky, USA). These films were processed with ImageJ software (National Institutes of Health, Bethesda, Maryland, USA).

2.3 Quantification of radiation dosage

In order to measure the radiation dose of patients after exposure to ionizing radiation, the effective dose of the patient was calculated based on the parameters of the devices. The parameters for iCT were taken after each scan and consist of the following: kV (kilovolt), mA (milliampere), mAs (milliampere per second), CTDI (computer tomography dose index) and DLP (dose length product). For the biplanar C-arms, the parameters were taken at the end of the surgery: kV, mA, DAP (dose area product), entrance dose and fluoroscopy time. After collection of the previous parameters, the effective dose was calculated by using a conversion factor, which was obtained by a Monte Carlo simulation. This simulation generated several scenarios based on average weight and length of a fictive patient, and the distance and angle of device to patient. The two conversion factors for the biplanar C-arms (AP: 0.032; L: 0.013) were multiplied with the reference dose, taking the distance into account, to calculate the effective dose. To obtain the total effective dose with the use of biplanar C-arms, a summation of the effective dose of the lateral and AP C-arm was done. For iCT,

the conversion factor (0.0105) was multiplied by the sum of all DLPs. The total effective dose for iCT is obtained by a summation of the effective dose of the iCT and the effective dose of the lateral C-arm, since the C-arm is used to place the graft cages during an iCT procedure.

The PSD (Peak Skin Dose) is measured by applying two Gafchromic™ films on the abdomen of the patient: one on the frontal abdomen and one on the lateral abdomen, on the side of the X-ray source. The Gafchromic™ films were calibrated and afterwards processed with Image J software.

To measure the radiation dose of staff, personal dosimeters were given to the surgeon, scrub nurse and anesthesiologist before onset of the surgery. The dosimeters were worn on top of the lead apron during the procedure. To read out the radiation doses, the DoseViewer software program was used. The accumulated absorbed effective dose was determined by marking the start and end time of the operation.

2.4 Set-up during surgical procedures

Depending on the imaging device used, the set-up and workflow of the operation differs. To determine the efficiency of the different imaging devices, the operating time was measured. We measured two different time intervals. As shown in Figure 6 below, the first interval started when anesthetics were administered and ended with initiation of decompression. This time analysis evaluates the set-up and screw placement between the two devices. The second interval started with first incision en ended with the last suture. This time analysis observes the total length of the procedure with exclusion of the set-up before the first incision.

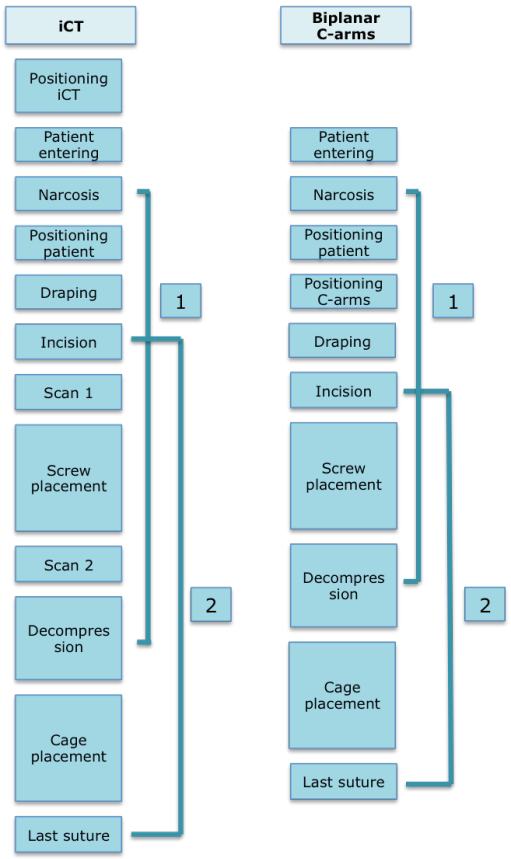

Figure 6: Schematic view of the efficiency measurement of the MI-PLIF procedure between iCT and

biplanar C-arms. The first timing interval starts at drug administration and ends at decompression. The second timing starts at first incision and ends at last suture. Note, the boxes do not represent the time used.

In the paragraphs below the set-up and workflow in the operating rooms during the MI-PLIF procedures will be further discussed in detail.

2.4.1 PLIF procedure with C-arm fluoroscopy

Before the patient entered, the dosimeters were distributed among the surgeon, nurse and anesthesiologist. After drug administration, the patient is turned in a prone position and the C-arms were positioned anterior-posteriorly and laterally of the patient. In order to determine the correct position, fluoroscopic images were taken. During this set-up, the length from patient to device and device angle were measured. The positions of the C-arms were marked on the ground and the operating field was sterilized. After draping, the trajectory of the screws was determined with the use of puncture needles and the biplanar C-arms. Next, K-wires were placed and the AP C-arm was removed from the operating field. The screws were placed over the K-wires with the use of solely the lateral C-arm. In the second part of the surgery, the disc is removed with the use of a microscope without fluoroscopy. The placement of the intervertebral cages was done with the use of the lateral C-arm. The staff wore a lead apron during the whole procedure.

2.4.2 PLIF procedure with Intraoperative CT

The PLIF procedure with the Airo® iCT was performed in a similar matter. Instead of positioning of the C-arms before sterilization of the patient, the Airo® was set-up before the patient entered the operating theatre. After drug administration to the patient, the patient was placed in a prone position and the operation field was sterilized. A reference frame was placed on the spinous process of a vertebra near the fusion level through a minimal midline incision. In order to maintain a sterile environment, an additional draping of the patient was performed. During the scanning period, staff left the operation room or hide behind a lead wall. After the scanning, the additional draping was removed and the lateral incisions were made for the placement of the screws. Meanwhile, the scans were automatically loaded into the neuronavigation Brainlab system. The screws were then placed under neuronavigation guidance. After the screw placement, the second scan was performed for intraoperative evaluation. During this scan, the staff left the operating room and the second scanning time was used to put on radiation protection gear such as a lead apron. The second part of the procedure, including the placement of the cages, was performed with a lateral C-arm. Therefore, the further procedure was identical as performed with the biplanar C-arms.

2.5 Statistical analysis

The one-sample Kolmogorov-Smirnov Test was used to test for normality. A student T-test and Mann-Whitney U test was used to compare normally and not normally distributed continuous data, retrospectively. Depending on normality, a Chi-squared test or Fischer's exact test was performed for categorical data. Correlation between the two continuous not-normal variables was calculated by a Spearman's correlation. A p-value of less than 0.05 was considered statistically significant. All statistical analysis were performed using SPSS Statistics Software 25.0 (IBM® Inc., Armonk, New York, USA).

3 Results

In the section below the results collected during this study are represented for the patient, staff and time efficiency.

3.1 Patient data

A total of 71 patients were recruited for this study. Of these, 14 were excluded due to the following reasons: incomplete ICF, conversion to open surgery, different C-arm device, no cage placement. Of the 57 included patients, 17 patients underwent a MI-PLIF with iCT and 40 patients underwent MI-PLIF with biplanar C-arms. Surgeon 1 operated on 15 patients (2 biplanar C-arm, 13 iCT); surgeon 2 operated on 13 patients (9 biplanar C-arm, 4 iCT) and surgeon 3 operated on 27 patients (27 biplanar C-arm). The mean age patients who underwent MI-PLIF with iCT was 60 years. For patients who underwent MI-PLIF with biplanar C-arms, the mean was 58 years. Operative indications were; listhesis (39), stenosis (19), discopathy (15), therapy resistant pain (4), recurrent herniation (6), facet arthritis (5) or sclerosis (1). Of these, 27 patients had several mixed indications. All demographic data and operative characteristics are summarized in Table 1. There were no significant statistical differences between the patient groups.

Table 1: Demographic data for patients who underwent MI-PLIF surgery with iCT compared to biplanar C-arms.

	iCT	Biplanar C-arms
No. patients (n)	17	40
Age, in years (mean ± SD)	58 (56-63)	55 (48-69)
BMI (median [IQR])	26,65 ± 5.07	27.01 ± 4.48
Gender (M/F) (% male)	6/11 (35.29)	16/24 (40.00)
Indications (no. [% of patients])		
Facet arthritis	/	5
Sclerosis	/	1
Listhesis	13	26
Stenosis	7	12
Discopathy	3	12
Therapy resistant pain	2	2
Hernia	3	3
Level fusion (no. [% of patients])		
Single level	16 (94.11)	35 (87,50)
Multi-level	1 (5.88)	5 (12.50)
Surgeon (no. [% of patients])		
Surgeon 1	13 (76.47)	2 (5.00)
Surgeon 2	4 (23.53)	9 (22.50)
Surgeon 3	0 (0)	27 (67.50)

SD = Standard Deviation, IQR = Interquartile Range, M = male, F = female.

3.2 Radiation dose of patient

To measure the exposure of the patients to radiation, two different radiation dosages were measured. In the first section, the PSD was represented for the lateral an anterior-posterior side of the patient. The second section represented the ED. A comparison between two imaging devices was done for these dosages.

3.2.1 Peak Skin Dose

The PSD was measured on the lateral and anterior-posterior side of the patient in order to compare the localized radiation dose on the skin of the patient for the biplanar C-arms and the iCT during a MI-PLIF procedure (Fig. 7)

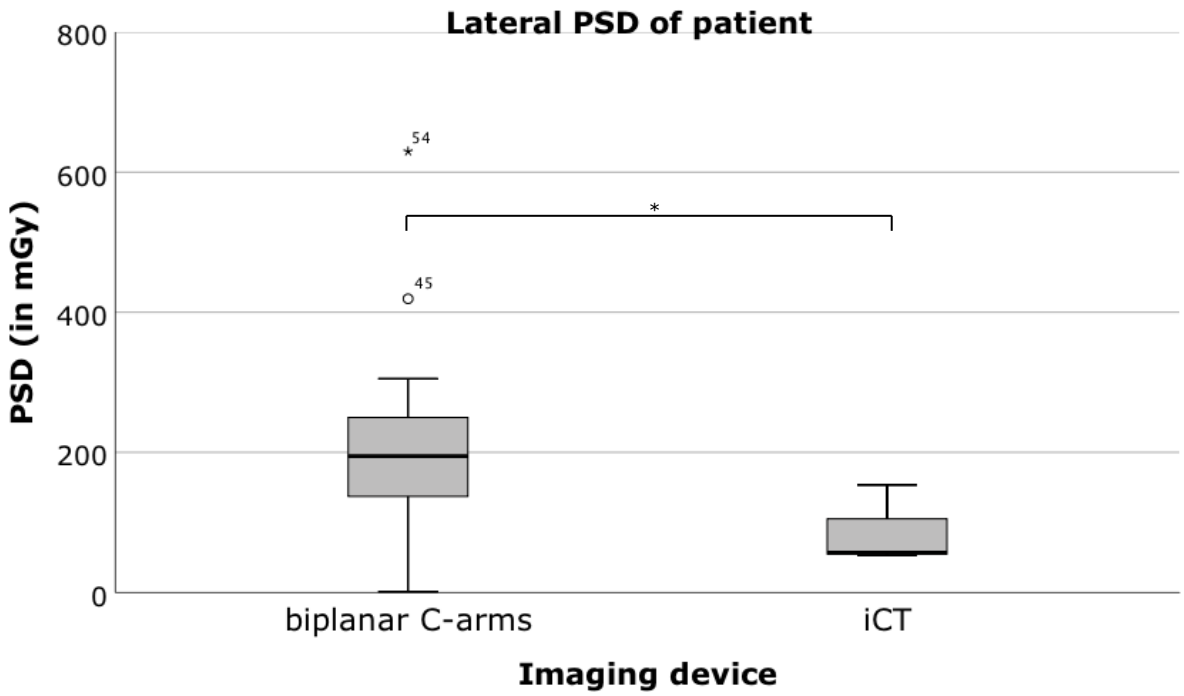

Figure 7: The lateral PSD of the patient during a MI-PLIF surgery compared between imaging devices. The lateral PSD of the patient (in mGy) compared between biplanar C-arms (n=24) and the iCT (n=3). Data was analyzed with a two-tailed T-Test Test after testing for normality with a Kolmogorov-Smirnov Test (* indicates p≤0.05). MI-PLIF: minimally invasive posterior lumbar interbody fusion; iCT: intraoperative CT; PSD: Peak Skin Dose; mGy: milli gray.

The lateral PSD of the patient encountered with a procedure performed with an iCT had a mean of 87.69 mGy ± 56.89. For procedures with biplanar C-arms, the mean effective dose was 210.76 mGy ± 123.57. Overall there was a significant difference between the biplanar lateral PSD and the iCT on a significance level of 5% (Fig. 7).

On the other hand, there was no significant difference for the anterior-posterior measurement of the PSD for the patient between the both imaging groups (Fig. 8). The median for this measurement of procedures performed with the biplanar C-arms was 46.35 mGy (20.79-58.82) and for procedures performed with iCT 47.29 mGy (40.27-50.01). Note the small interquartile range for the iCT PSD measurements.

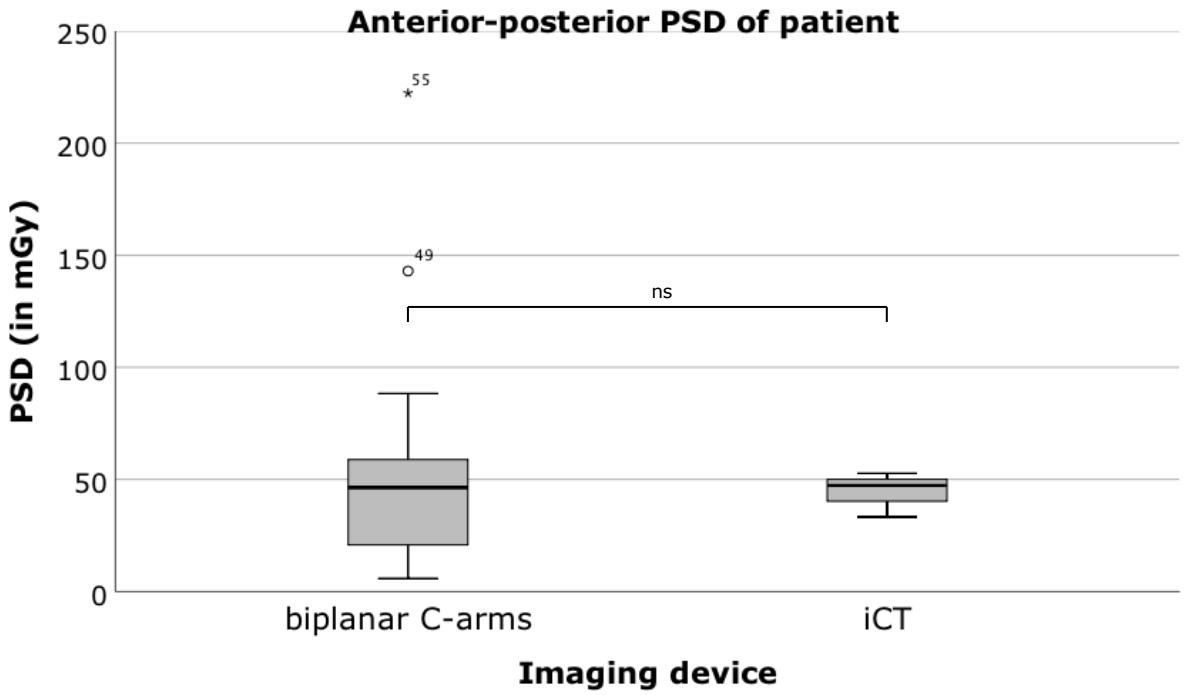

Figure 8: The anterior-posterior PSD of the patient during a MI-PLIF surgery compared between imaging devices. The anterior-posterior PSD of the patient (in mGy) compared between biplanar C-arms (n=24) and the iCT (n=3). Data was analyzed with a Mann-Whitney U Test after testing for normality with a Kolmogorov-Smirnov Test (ns indicates p>0.05). MI-PLIF: minimally invasive posterior lumbar interbody fusion; iCT: intraoperative CT; PSD: Peak Skin Dose; mGy: milli gray.

3.2.2 Effective Dose

The ED was used to evaluate the dose patients are exposed to during a MI-PLIF procedure. The median of the effective dose patients encountered with a procedure performed with iCT was 8.59 mSv (4.21-10.45). For procedures with biplanar C-arms, the median effective dose was 2.14 mSv (1.27-2.98). Figure 9 shows a significantly lower ($p<0.001$) ED of the patient in MI-PLIF procedures performed with the use of biplanar C-arms compared to iCT. However, note the broad range of values with biplanar C-arm results due to several outliers.

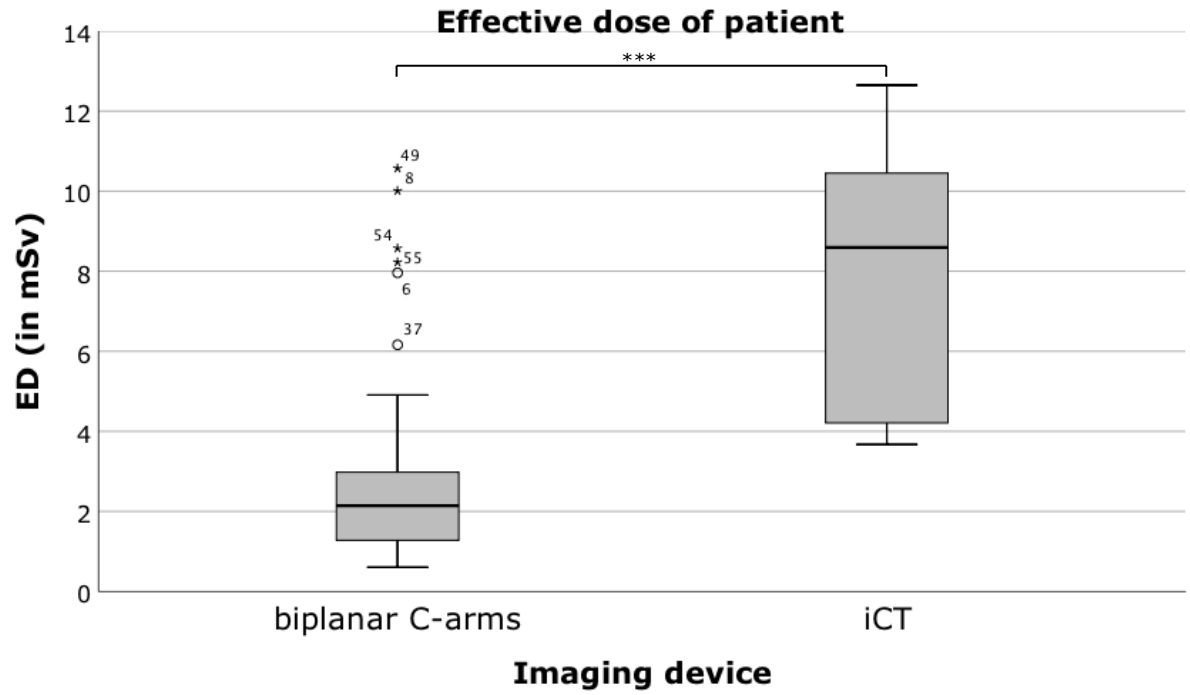

Figure 9: The effective dose of the patient during a MI-PLIF surgery compared between imaging devices. The effective dose of the patient (in mSv) compared between biplanar C-arms (n=38) and the iCT (n=14). Data was analyzed with a Mann-Whitney U Test after testing for normality with a Kolmogorov-Smirnov Test (*** indicates p≤0.001). MI-PLIF: minimally invasive posterior lumbar interbody fusion; iCT: intraoperative CT; ED: Effective Dose; mSv: milli sievert.

3.2.3 Correlation between BMI and ED

To evaluate if the radiation dose increases with size, a correlation of the ED and the BMI of the patients was performed (Fig. 10). There was no significant correlation between ED and BMI. However, there was a slight positive linear correlation.

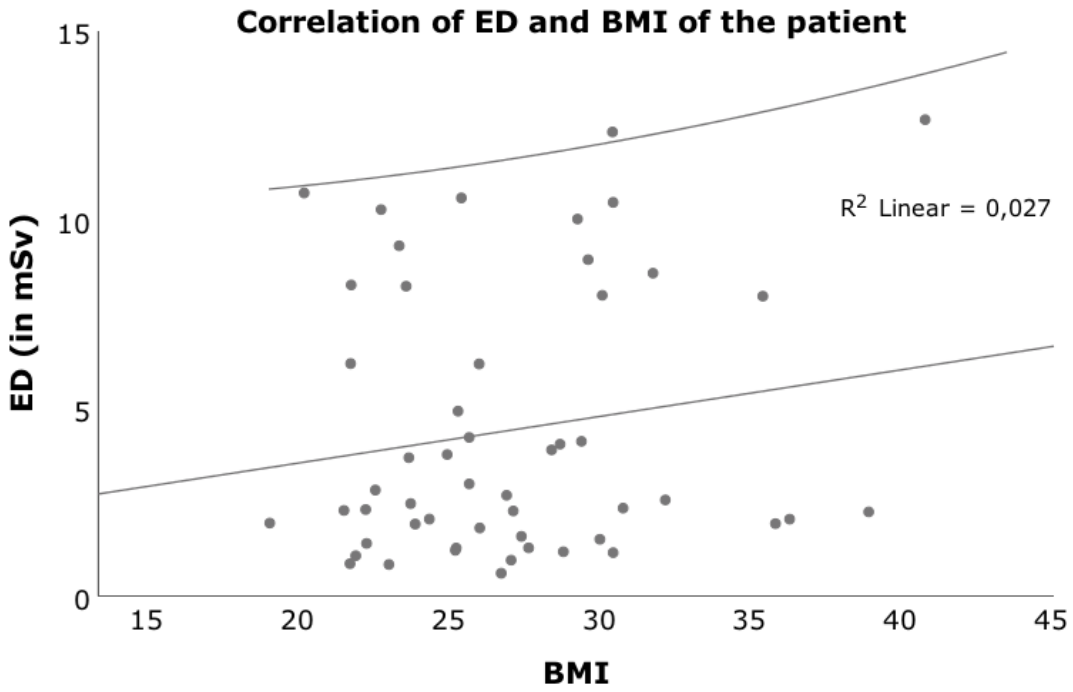

Figure 10: The correlation of the ED and BMI of the patient during a MI-PLIF surgery. The effective dose of the patient (in mSv) plotted versus the BMI of the patient (n=52) with a confidence level of 95%. Data was analyzed with a Spearman correlation after testing for normality with a Kolmogorov-Smirnov Test. MI-PLIF: minimally invasive posterior lumbar interbody fusion; iCT: intraoperative CT; ED: Effective Dose; BMI: Body Mass Index; mSv: milli sievert.

3.3 Radiation dose of staff during MI-PLIF surgery

In order to evaluate the radiation dose to which staff was exposed, the ED was measured for the surgeon, the scrub nurse and the anesthesiologist. The surgeon received a median effective dose of 8 μSv (5-24) during a procedure performed with an iCT. For procedures with biplanar C-arms, the median effective dose was 135.5 μSv (58-228) for the surgeon. This was a statistically significant difference ($p \leq 0.001$), with higher doses during the C-arm procedure. The results are shown in Figure 11.

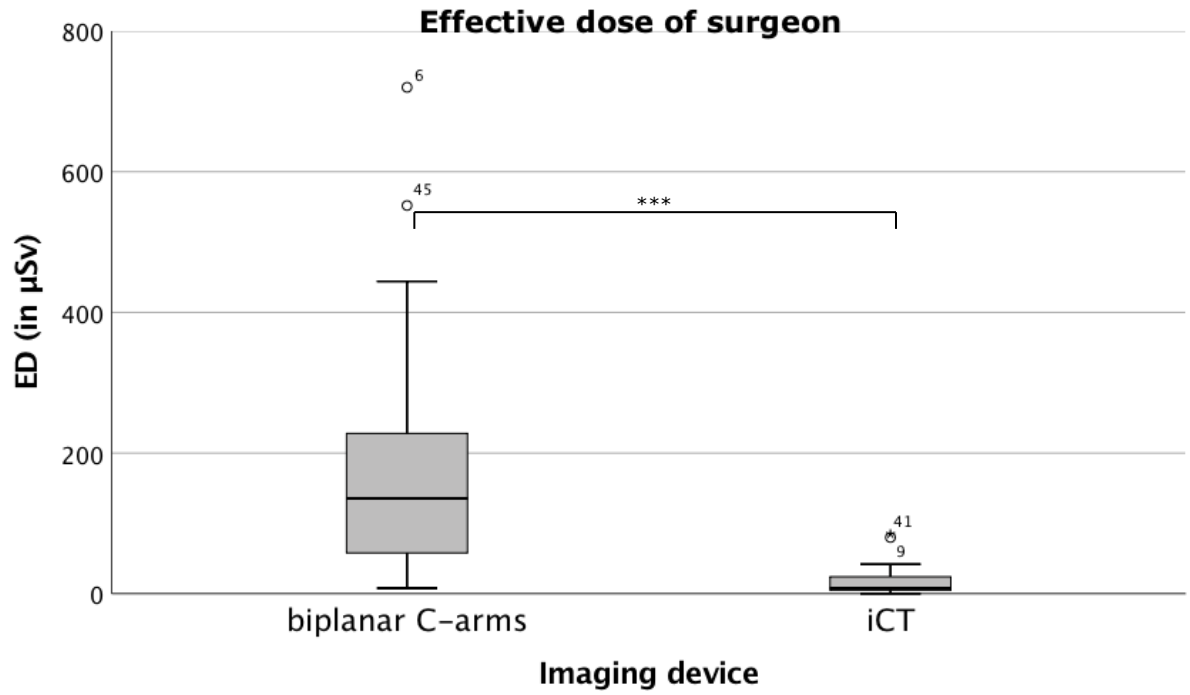

Figure 11: The effective dose of the surgeon during a MI-PLIF surgery compared between imaging devices. The effective dose of the surgeon (in **µ**Sv) compared between biplanar C-arms (n=38) and the iCT (n=17). Data was analyzed with a Mann-Whitney U Test after testing for normality with a Kolmogorov-Smirnov Test (*** indicates p≤0.001). MI-PLIF: minimally invasive posterior lumbar interbody fusion; iCT: intraoperative CT; ED: Effective Dose; **µ**Sv: micro sievert.

For the nurse, the dosages were at a lower range compared to the dosages of the surgeon. The effective dose median for the nurse was 6 µSv (3-15.5) for a procedure performed with biplanar C-arms (Fig. 12). The effective dose with a procedure with iCT had a significant lower (p≤0.001) dose of 1 µSv (0-3) compared to the biplanar C-arm procedure (Fig. 12).

The lowest dosages of the staff members were observed for the anesthesiologist. The effective dose medians were 0 µSv (0-1) and 1 µSv (0-2.5), respectively for iCT and biplanar C-arm procedures (Fig. 13). There was no significant difference detected between the both imaging device groups.

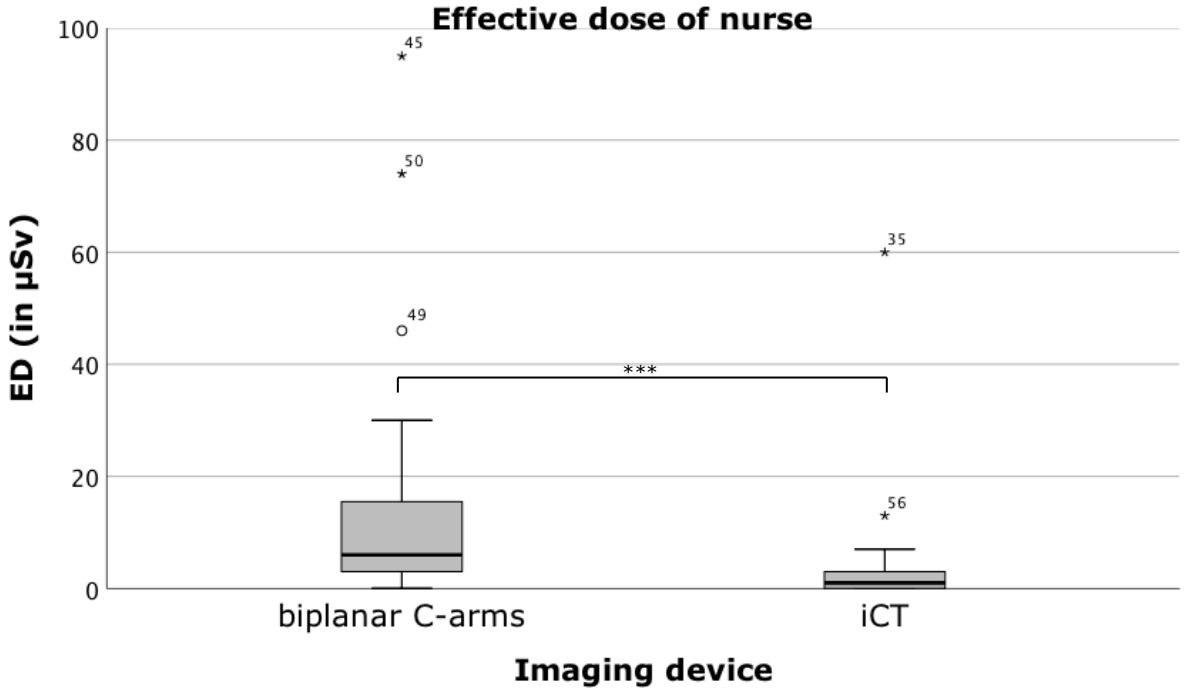

Figure 12: The effective dose of the nurse during a MI-PLIF surgery compared between imaging devices. The effective dose of the nurse (in µSv) compared between biplanar C-arms (n=39) and the iCT (n=17). Data was analyzed with a Mann-Whitney U Test after testing for normality with a Kolmogorov-Smirnov Test (*** indicates p≤0.001). MI-PLIF: minimally invasive posterior lumbar interbody fusion; iCT: intraoperative CT; ED: Effective Dose; µSv: micro sievert.

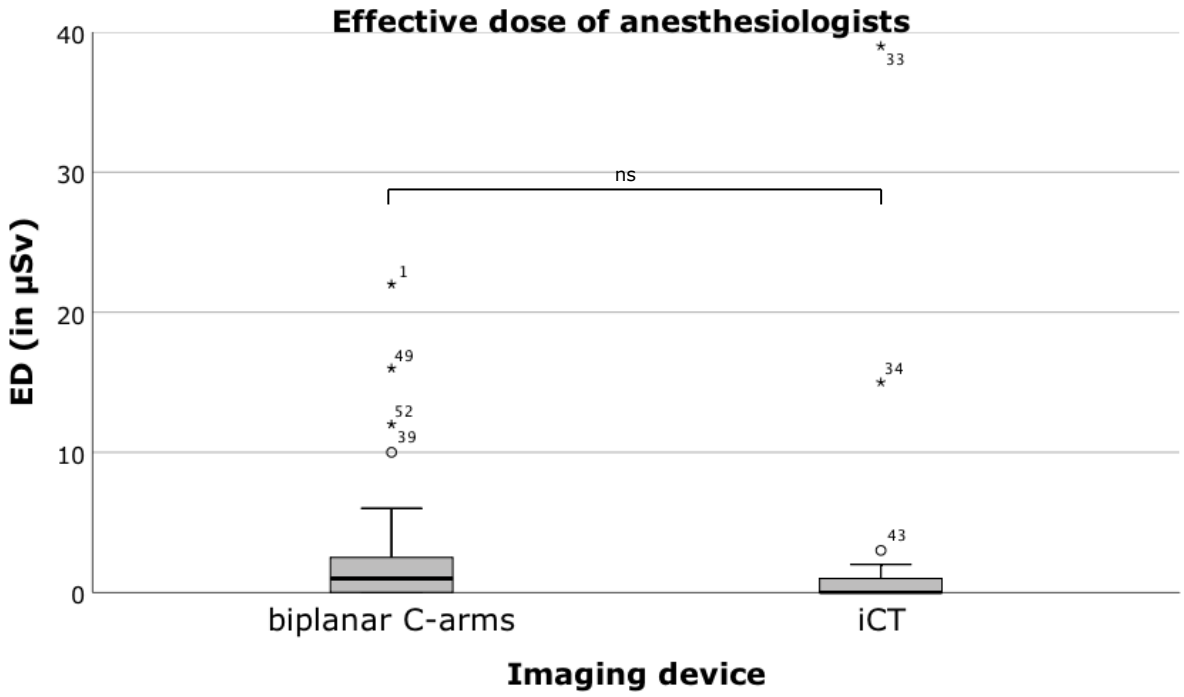

Figure 13: The effective dose of the anesthesiologist during a MI-PLIF surgery compared between imaging devices. The effective dose of the anesthesiologist (in µSv) compared between biplanar C-arms (n=39) and the iCT (n=17). Data was analyzed with a Mann-Whitney U Test after testing for normality with a Kolmogorov-Smirnov Test (ns indicates p>0.05). MI-PLIF: minimally invasive posterior lumbar interbody fusion; iCT: intraoperative CT; ED: Effective Dose; µSv: micro sievert.

3.4 Efficiency of imaging devices

To evaluate the efficiency of the imaging devices used during the MI-PLIF procedures, two time intervals were measured (Fig. 14).

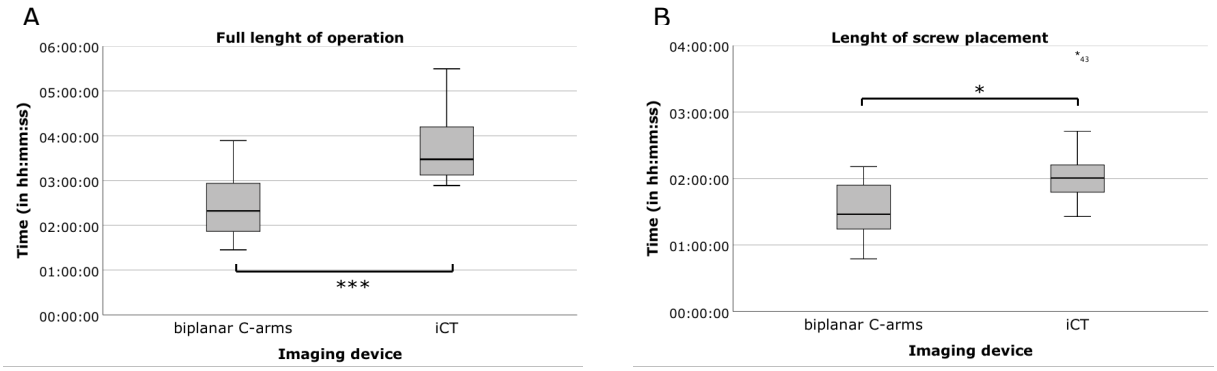

Figure 14: Time intervals during a MI-PLIF surgery compared between imaging devices. (A) Full length of MI-PLIF surgery from first incision to last suture (in hh:mm:ss) compared between biplanar C-arms (n=40) and the iCT (n=17). **(B)** Length of screw placement during MI-PLIF surgery from narcosis to decompression incision/bone removal (in hh:mm:ss) compared between biplanar C-arms (n=12) and iCT (n=11). Data was analyzed with a two-tailed T-test after testing for normality with a Kolmogorov-Smirnov Test (*** indicates p≤0.001, ** indicates p<0.01, * indicates p<0.05). MI-PLIF: minimally invasive posterior lumbar interbody fusion; iCT: intraoperative CT.

The mean of the measurement of the length of screw placement with iCT (n=11) was 2:08:20 ± 0:40:55. In comparison, the mean of the measurement of the length of screw placement with biplanar C-arms (n=12) was 1:31:12 ± 0:25:39. There was a significant difference (p=0.020) between the time intervals for screw placement as shown in Figure 14.

For the measurement of the full length of the surgery the mean with iCT (n=17) was 3:44:11 ± 0:42:04. Remarkebly, the mean of the measurement of the full length of the surgery with biplanar C-arms was 2:29:04 ± 0:41:23. In Figure 14A, the total time of the operation is significantly shorter (p=0.000) the time for iCT.

Taken together, the iCT has for both intervals a significantly longer operation time than the biplanar C-arm. Note, there is a lower significance level for the screw placement interval.

4 Discussion

The aim of this study was to assess the radiation dosages, to which patients and staff were exposed to during MI-PLIF procedures, using biplanar C-arms versus intraoperative CT as neuronavigation device. The importance of investigating the radiation exposure is supported by the ICRP, stating the ALARA principle that radiation doses to patients and staff should be kept as low as reasonably achievable (19). So far, the radiation exposure to patients and staff is poorly studied for the newly developed mobile Airo® iCT. We analyzed the radiation doses of patients by assessing the peak skin dose (PSD) and effective dose (ED), and the doses for staff by assessing the ED with personal dosimeters. Moreover, we analyzed the time efficiency of procedures with both imaging devices. Our results provided some interesting observations.

Radiation exposure to patient

An important observation in our study is the significant lower PSD on the lateral side of the patient during the MI-PLIF procedures with iCT. The present data indicate that iCT has a larger radiation area with a lower localized dose, while C-arm fluoroscopy results in a localized radiation area with a higher focal dose. Moreover, the large variability concerning the PSD in C-arm fluoroscopy suggests that the radiation is dependent on several other factors, such as the surgeon performing the surgery or the complexity of the procedure. A comparison with the literature is difficult since radiation doses can differ depending on the procedure, the imaging device used and the measuring technique. In this study PSD doses were measured with the use of Gafchromic™ films, since a calculation of the entrance dose at the skin is not accurate due to the changes in distance from device to patient during the procedure. Bindal *et al.* described a skin exposure during a MI-TLIF procedure with C-arm fluoroscopy of 59.5 mGy (8.3-252) and 78.8 mGy (6.3-269.5) to the patient's skin, for in the AP and lateral plane respectively (20). The results in our study for a MI-PLIF with C-arm fluoroscopy showed a PSD of 46.4 mGy (20.8-58.8) and 210.8 mGy ± 123.6 on the AP and L side, respectively. These doses are reasonably low and do not exceed the threshold of 2 Gy determined by the ICRP associated with deterministic effects of the skin, such as erythema. Although the doses are well below the limit of the ICRP for deterministic effects, the stochastic effects of low-dose radiation are still not well understood (21).

Another evaluation of the patient's radiation exposure was done with the calculation of the ED. Thereby, the outcomes showed that iCT increased the overall ED of the patient by fourfold compared with the conventional biplanar C-arms. It can be argued that a postoperative CT scan in the medical imaging department of approximately the same ED as two iCT scans equalizes the radiation exposure for the patient in the fluoroscopy group. However, in practice, the postoperative CT scan is not consistently performed, unless the surgeon suspects malposition of the pedicle screws. During this study, in the iCT group, the surgeons evaluated the screw placement intraoperatively by a second CT scan during the procedure. Mendelsohn *et al.* stated that there is no need for the second scan (22). Besides, the accuracy of the screw placement is higher with neuronavigation (23). Therefore, it should be considered that the surgeon evaluates the probability of screw malposition before administration of additional radiation dose to the patient. Moreover, Navarro-Ramirez *et al*. have demonstrated that the cage placement can also be performed with an

iCT scan and neuronavigation (24, 25). In our study, the surgeons used the lateral C-arm for the cage placement in the iCT study group. These two factors represent points of interest for the surgeon in reducing the radiation dose for patients.

A third factor that may influence the patient's radiation dose is BMI. Surprisingly, there was no significant correlation found in this study between the ED and the BMI of the patient. This finding was unexpected since it is in contrast to previous studies, which have suggested that there was a significant correlation (24, 26). A possible explanation for this might be that the radiation dose was also influenced by other factors such as the surgeon performing the procedure and the difficulty of the procedure.

Radiation exposure to staff

The radiation exposure to staff was significantly lower in the procedures performed with iCT compared to biplanar C-arms. Specifically the median of the ED for the surgeon was almost 17 times lower in the iCT group. For the nurse, the median ED would lower 6 times with iCT. The results of this study did not show any significant difference in radiation dose for the anesthesiologist. This is because the anesthesiologist is further removed from the operating field and scatter radiation decreases with an increase in distance from the patient (27). Although the groups are not equally balanced, the ED for staff in general is very low in the iCT study group. This is of great importance since surgeons receive 4.2% of the total radiation emitted from the patient according to Mulconrey *et al.* (28). Taking the lead shielding into account, the surgeon would receive 0.25% of the patient's radiation (29). Moreover, this is of particular interest since previous studies have showed that thoracolumbar spinal surgeons have a 10 to 12 times higher exposure during fluoroscopic procedures as surgeons performing non-spinal musculoskeletal procedures (30). From the point of view of the staff in the operating theatre, the iCT is a suitable device for neuronavigation, as repetitive exposure to radiation may lead to radiation related conditions, such as dermatitis and cataract. Since, leaded glasses and gloves are impractical, these are often not used during the procedures, leaving some body parts such as the eyes and hands unprotected. Several studies investigated the effect of ionizing radiation on the eyes, but still there is little awareness for the exposure of such a radiosensitive tissue (31, 32). Taher *et al.* determined the radiation exposure of the surgeon during a MI-LLIF procedure (33). This study measured an ED of 26.4 μSv and 146.2 μSv in the surgeon's eyes and hands, respectively. Furthermore, they stated that they could perform 2700 MI-LLIF procedures per year before exceeding the ICRP limits (33). In comparison, we could perform 2500 MI-PLIF procedures with iCT and 147 MI-PLIF procedures with C-arm fluoroscopy, before exceeding the dose limits for the surgeon of 20 mSV per year. Thereby, staff can leave the operating room during the scanning period and therefore, there is no need to wear other protection gear such as lead aprons. This can result in fewer ergonomic complains such as back pain and muscular fatigue, caused by the weight of the gear on the shoulder and back during procedures of several hours (34, 35). In conclusion, iCT is a promising device for decreasing the health risks of staff with careful notion of the patient doses.

Evaluation of the efficiency

The results of this study showed a significant increase in full operation length and length of screw placement with iCT. For the evaluation of the full operation length, the average difference was one hour between both groups. When solely evaluating the duration for the screw placement, the procedure performed with iCT was on average 37 minutes longer than the procedure with fluoroscopy. For the evaluation of the screw placement, the significant difference was less pronounced and therefore it can be speculated that the significant difference in time is due to other factors. For example, it can be argued that the significant difference of the screw placement interval is due to time loss during calibration of the surgical instruments for the neuronavigation. Several studies suggest that the operation time with intraoperative navigation is strongly dependent on the steep learning curve of staff (36-39). A routine use of spinal navigation is therefore critical to overcome the learning curve. Furthermore, Khanna *et al.* suggested that besides the learning curve, the operation time can be shortened by performing a single scan (39). Since, the second part of the surgery is identical in procedures performed with both imaging devices and there is a less pronounced significance in the screw placement interval, the significant difference of the total operation length can be dependent on the surgeon, difficulty of the procedure or other factors.

Limitations

This study has some limitations. The first limitation is the unbalanced groups of the imaging devices; C-arm fluoroscopy and iCT. Thereby, the procedures were not evenly distributed among surgeons. Furthermore, the three surgeons may have positively biased accuracy and time intervals because of their profound experience. Besides, data was collected by two senior interns, which may result in a slight difference in recording of the time intervals.

Future

In the future the radiation dosages can possibly be lowered during an iCT procedure. The first option is a total navigation of the surgery with iCT, whereby a fluoroscopy device can be present at all times to check in case of doubt. Secondly, the radiation exposure of the patient should be carefully monitored to maintain within safety limits according to the ICRP. One option can be that the nurse reports to the surgeon when a certain level of radiation dose is reached. The use of standardized protocols in the future can reduce the radiation doses of the patient as well. The iCT software gives the option to choose several different radiation protocols based on the installed tube current. For example, if the first CT scan would be taken with a 75% protocol and the second scan with a 25% protocol, this will result in the first scan to be taken at 82.5 mA and the second scan at 27.5 mA compared to a maximum of 110 mA. Note that a lower tube current leads to a lower radiation dose and a lower image quality, thereby leaving it up to the surgeon which image quality is acceptable. Furthermore, surgeons should be aware of the high-exposure of the body and hands when using fluoroscopy devices and thereby adjust their position upon taking images. In order to protect the eyes, the surgeon can turn away or wear protective glasses. Besides, the use of iCT is very interesting in complicated instrumentations such as fixations or fusions in the cranio-cervical and cervico-thoracic junction, thoracic instrumentations with small pedicles and revision surgeries with loss of normal anatomic landmarks (40). These are procedures where high resolution 3D

imaging aids in the surgical orientation. In conclusion, iCT is a promising device if dealt with some issues.

It would be recommended to further precede this study in order to balance the different groups to increase statistical power. Moreover, it would be interesting to encounter the post-operative complications between the imaging devices. Furthermore, a cost-benefit analysis should be done, including the clinical outcomes, complications and revision surgeries.

5 Conclusion

The iCT is an interesting neuronavigation device for operating personnel to reduce and possibly eliminate radiation exposure in MI-PLIF procedures. However, the radiation dose for the patient is higher compared to the conventional biplanar C-arms. Therefore, a completely navigated procedure with the elimination of a second scan and standardization of the scan protocols should be further tested in order to reduce patient dosages. Besides, staff should be trained on working with the Airo® iCT in order to reduce operation time.

6 References

1. Nadeau M, Rosas-Arellano MP, Gurr KR, Bailey SI, Taylor DC, Grewal R, et al. The reliability of differentiating neurogenic claudication from vascular claudication based on symptomatic presentation. Can J Surg. 2013;56(6):372-7.
2. Mobbs RJ, Phan K, Malham G, Seex K, Rao PJ. Lumbar interbody fusion: techniques, indications and comparison of interbody fusion options including PLIF, TLIF, MI-TLIF, OLIF/ATP, LLIF and ALIF. J Spine Surg. 2015;1(1):2-18.
3. Deane JA, McGregor AH. Current and future perspectives on lumbar degenerative disc disease: a UK survey exploring specialist multidisciplinary clinical opinion. BMJ Open. 2016;6(9):e011075.
4. Kaiser MG, Eck JC, Groff MW, Watters WC, 3rd, Dailey AT, Resnick DK, et al. Guideline update for the performance of fusion procedures for degenerative disease of the lumbar spine. Part 1: introduction and methodology. J Neurosurg Spine. 2014;21(1):2-6.
5. Mobbs RJ, Sivabalan P, Li J. Minimally invasive surgery compared to open spinal fusion for the treatment of degenerative lumbar spine pathologies. J Clin Neurosci. 2012;19(6):829-35.
6. Karhade AV VV, Pompeu YA and Lu Y. Image Guided Spine Surgery: Available Technology and Future Potential. Austin Neurosurg Open Access. 2016;3(1):1043.
7. Wu AM, Chen CH, Shen ZH, Feng ZH, Weng WQ, Li SM, et al. The Outcomes of Minimally Invasive versus Open Posterior Approach Spinal Fusion in Treatment of Lumbar Spondylolisthesis: The Current Evidence from Prospective Comparative Studies. Biomed Res Int. 2017;2017:8423638.
8. A.J.J. Bos F.S. Draaisma WJCO, C.E. Rasmussen. Inleiding tot de stralingshygiëne. Maarssen: Elsevier; 2000.
9. Graham DT CP, Vosper M. Principles of radiological physics. 5th ed. Edinburgh: Churchill Livingstone2006.
10. Bushberg JT SJ, Leidholdt EM, Boone JM. The essential physics og medical imaging. Third ed: Lippincott Williams & Wilkens, a Wolters Kluwer business; 2012.
11. Healthcare G. GE OEC Fluorostar Mobile Digital C-Arm: Operator Manual. UT, USA2015.
12. Das CJ, Baliyan V, Sharma S. Image-guided urological interventions: What the urologists must know. Indian J Urol. 2015;31(3):202-8.
13. AG B. Spine Navigation Brochure. Munich, Germany2017.
14. Mobius Imaging L. Airo Mobile CT-System: Operating Manual. MA, USA2016.
15. Mobius Imaging L. Airo-System: Application Guide Protocols Principles. MA, USA2018.
16. Lee JKT SS, Stanley RJ, Heiken JP. Computed Body Tomography with MRI Correlation. 4 ed: Lippincott Williams & Wilkins; 2006.
17. Radiologykey. Image production 2016 [updated Feb 27. Available from: https://radiologykey.com/image-production/.
18. Weissleder R WJ, Harisinghani MG, Chen JW. Primer of Diagnostic Imaging. 5 ed. MO,USA: Elsevier Mosby; 2011.
19. FANC. ARBIS 2017 [Available from: https://fanc.fgov.be/nl.
20. Bindal RK, Glaze S, Ognoskie M, Tunner V, Malone R, Ghosh S. Surgeon and patient radiation exposure in minimally invasive transforaminal lumbar interbody fusion. J Neurosurg Spine. 2008;9(6):570-3.
21. Averbeck D, Salomaa S, Bouffler S, Ottolenghi A, Smyth V, Sabatier L. Progress in low dose health risk research: Novel effects and new concepts in low dose radiobiology. Mutat Res. 2018;776:46-69.
22. Mendelsohn D, Strelzow J, Dea N, Ford NL, Batke J, Pennington A, et al. Patient and surgeon radiation exposure during spinal instrumentation using intraoperative computed tomography-based navigation. Spine J. 2016;16(3):343-54.
23. Luther N, Iorgulescu JB, Geannette C, Gebhard H, Saleh T, Tsiouris AJ, et al. Comparison of navigated versus non-navigated pedicle screw placement in 260 patients and 1434 screws: screw accuracy, screw size, and the complexity of surgery. J Spinal Disord Tech. 2015;28(5):E298-303.
24. Navarro-Ramirez R, Lang G, Lian X, Berlin C, Janssen I, Jada A, et al. Total Navigation in Spine Surgery; A Concise Guide to Eliminate Fluoroscopy Using a Portable Intraoperative Computed Tomography 3-Dimensional Navigation System. World Neurosurg. 2017;100:325-35.
25. Lian X, Navarro-Ramirez R, Berlin C, Jada A, Moriguchi Y, Zhang Q, et al. Total 3D Airo(R) Navigation for Minimally Invasive Transforaminal Lumbar Interbody Fusion. Biomed Res Int. 2016;2016:5027340.
26. Funao H, Ishii K, Momoshima S, Iwanami A, Hosogane N, Watanabe K, et al. Surgeons' exposure to radiation in single- and multi-level minimally invasive transforaminal lumbar interbody fusion; a prospective study. PLoS One. 2014;9(4):e95233.

27. Lee K, Lee KM, Park MS, Lee B, Kwon DG, Chung CY. Measurements of surgeons' exposure to ionizing radiation dose during intraoperative use of C-arm fluoroscopy. Spine (Phila Pa 1976). 2012;37(14):1240-4.
28. Mulconrey DS. Fluoroscopic Radiation Exposure in Spinal Surgery: In Vivo Evaluation for Operating Room Personnel. Clin Spine Surg. 2016;29(7):E331-5.
29. Ahn Y, Kim CH, Lee JH, Lee SH, Kim JS. Radiation exposure to the surgeon during percutaneous endoscopic lumbar discectomy: a prospective study. Spine (Phila Pa 1976). 2013;38(7):617-25.
30. Rampersaud YR, Foley KT, Shen AC, Williams S, Solomito M. Radiation exposure to the spine surgeon during fluoroscopically assisted pedicle screw insertion. Spine (Phila Pa 1976). 2000;25(20):2637-45.
31. Milacic S. Risk of occupational radiation-induced cataract in medical workers. Med Lav. 2009;100(3):178-86.
32. Vano E, Kleiman NJ, Duran A, Rehani MM, Echeverri D, Cabrera M. Radiation cataract risk in interventional cardiology personnel. Radiat Res. 2010;174(4):490-5.
33. Taher F, Hughes AP, Sama AA, Zeldin R, Schneider R, Holodny EI, et al. 2013 Young Investigator Award winner: how safe is lateral lumbar interbody fusion for the surgeon? A prospective in vivo radiation exposure study. Spine (Phila Pa 1976). 2013;38(16):1386-92.
34. Moore B, vanSonnenberg E, Casola G, Novelline RA. The relationship between back pain and lead apron use in radiologists. AJR Am J Roentgenol. 1992;158(1):191-3.
35. Orme NM, Rihal CS, Gulati R, Holmes DR, Jr., Lennon RJ, Lewis BR, et al. Occupational health hazards of working in the interventional laboratory: a multisite case control study of physicians and allied staff. J Am Coll Cardiol. 2015;65(8):820-6.
36. Bai YS, Zhang Y, Chen ZQ, Wang CF, Zhao YC, Shi ZC, et al. Learning curve of computer-assisted navigation system in spine surgery. Chin Med J (Engl). 2010;123(21):2989-94.
37. Hecht N, Kamphuis M, Czabanka M, Hamm B, Konig S, Woitzik J, et al. Accuracy and workflow of navigated spinal instrumentation with the mobile AIRO((R)) CT scanner. Eur Spine J. 2016;25(3):716-23.
38. Nottmeier EW, Crosby TL. Timing of paired points and surface matching registration in three-dimensional (3D) image-guided spinal surgery. J Spinal Disord Tech. 2007;20(4):268-70.
39. Khanna AR, Yanamadala V, Coumans JV. Effect of intraoperative navigation on operative time in 1-level lumbar fusion surgery. J Clin Neurosci. 2016;32:72-6.
40. Hartl R, Lam KS, Wang J, Korge A, Kandziora F, Audige L. Worldwide survey on the use of navigation in spine surgery. World Neurosurg. 2013;79(1):162-72.

Auteursrechtelijke overeenkomst

Ik/wij verlenen het wereldwijde auteursrecht voor de ingediende eindverhandeling:
Radiation exposure during posterior lumbar intervertebral fusion procedures, using intraoperative CT versus conventional C-arms

Richting: **Master of Biomedical Sciences-Clinical Molecular Sciences**
Jaar: **2018**

in alle mogelijke mediaformaten, - bestaande en in de toekomst te ontwikkelen - , aan de Universiteit Hasselt.

Niet tegenstaand deze toekenning van het auteursrecht aan de Universiteit Hasselt behoud ik als auteur het recht om de eindverhandeling, - in zijn geheel of gedeeltelijk -, vrij te reproduceren, (her)publiceren of distribueren zonder de toelating te moeten verkrijgen van de Universiteit Hasselt.

Ik bevestig dat de eindverhandeling mijn origineel werk is, en dat ik het recht heb om de rechten te verlenen die in deze overeenkomst worden beschreven. Ik verklaar tevens dat de eindverhandeling, naar mijn weten, het auteursrecht van anderen niet overtreedt.

Ik verklaar tevens dat ik voor het materiaal in de eindverhandeling dat beschermd wordt door het auteursrecht, de nodige toelatingen heb verkregen zodat ik deze ook aan de Universiteit Hasselt kan overdragen en dat dit duidelijk in de tekst en inhoud van de eindverhandeling werd genotificeerd.

Universiteit Hasselt zal mij als auteur(s) van de eindverhandeling identificeren en zal geen wijzigingen aanbrengen aan de eindverhandeling, uitgezonderd deze toegelaten door deze overeenkomst.

Voor akkoord,

Houben, Elien

Datum: **8/06/2018**